ACS APPLIED MATERIALS & INTERFACES

Research Article

www.acsami.org

FAS Grafted Electrospun Poly(vinyl alcohol) Nanofiber Membranes with Robust Superhydrophobicity for Membrane Distillation

Zhe-Qin Dong, Bao-Juan Wang, Xiao-hua Ma, Yong-Ming Wei, and Zhen-Liang Xu*

State Key Laboratory of Chemical Engineering, Membrane Science and Engineering R&D Lab, Chemical Engineering Research Center, Shanghai Key laboratory of Mutiphase Materials Chemical Engineering, East China University of Science and Technology (ECUST), 130 Meilong Road, Shanghai 200237, China

Supporting Information

ABSTRACT: This study develops a novel type of electrospun nanofiber membranes (ENMs) with high permeability and robust superhydrophobicity for membrane distillation (MD) process by mimicking the unique unitary microstructures of ramee leaves. The superhydrophobic ENMs were fabricated by the eletrospinning of poly(vinyl alcohol) (PVA), followed by chemical cross-linking with glutaraldehyde and surface modification via low surface energy fluoroalkylsilane (FAS). The resultant FAS grafted PVA (F-PVA) nanofiber membranes were endowed with self-cleaning properties with water contact angles of 158° and sliding angles of 4° via the modification process, while retaining their high porosities and interconnected open structures. For the first time, the robust superhydrophobicity of the ENMs for MD was confirmed by testing the F-PVA nanofiber membranes under violent ultrasonic treatment and harsh chemical conditions. Furthermore, vacuum membrane distillation experiments illustrated that the F-PVA membranes presented a high and stable permeate flux of 25.2 kg/m^{2}h, 70% higher than those of the commercial PTFE membranes, with satisfied permeate conductivity (<5 μm/cm) during a continuous test of 16 h (3.5 wt % NaCl as the feed solution, and feed temperature and permeate pressure were set as 333 K and 9 kPa, respectively), suggesting their great potentials in myriad MD processes such as high salinity water desalination and volatile organiccompounds removal.

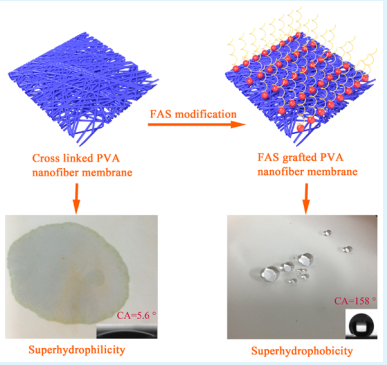

KEYWORDS: *superhydrophobicity, membrane distillation, eletrospinning, poly(vinyl alcohol), nanofiber membrane*

1. INTRODUCTION

With the ever increasing demand for freshwater resources, seawater desalination has received considerable attention in recent years.[1,2] Among various desalination technologies, membrane distillation (MD) is an attractive alternative for water desalination with the merits of simple configuration, mild operation and high rejection of salts.[3−6] In MD, the hydrophobic membrane servers as a barrier that allows only vapor to pass through, and therefore its properties have great influence on the performance of MD process. Typically, the porosity and pore size of a membrane should be appropriately designed for attaining high permeate flux and desirable salt rejection.[7] Furthermore, the membrane surface should be hydrophobic or preferably superhydrophobic to avoid pore wetting in long-term stage.[8] However, most of the membranes employed in MD are initially used for microfiltration and their structure and surface are not specially designed.[9] As a result, the development of membranes with highly hydrophobicity, high porosity, and good stability that can fulfill the potentials of MD process is highly desired.

Recently, electrospinning has been recognized as an advanced technology for the fabrication of MD membranes.[10−13] Compared with conventional membranes, the electrospun nanofiber membranes (ENMs) are promising in the MD applications with the prominent advantages of high hydrophobicity, high void volume fraction, and controllable pore size. Feng et al.[14] first explored the feasibility of polyvinylidene fluoride (PVDF) ENMs in MD, and their results showed that the PVDF ENMs presented a salt rejection over 99% with a permeate flux comparable to those of commercial microfiltration membranes, which promised the potentials of PVDF ENMs in MD. In the study of Liao et al.,[15] the optimized PVDF ENMs via adjusting electrospinning parameters and post treatment exhibited a permeate flux better than commercial microfiltration membranes. Unfortunately, the resultant PVDF ENMs only possessed a low liquid entry pressure of water (LEPw) of 35 kPa because of their loosely packed membrane structures, which makes the ENMs readily able to be wetted and thus limits their practical applications in MD.

The pore wetting issue of ENMs in MD can be alleviated either by decreasing pore size or increasing surface hydrophobicty.[12] Because decreased pore size would result in lower permeability, much effort has been engaged in the preparation of superhydrophobic ENMs by mimicking the hierarchical structure of louts leaves.[16−19] In our previous study,[16] the

Received: August 12, 2015
Accepted: September 26, 2015
Published: September 27, 2015

DOI: 10.1021/acsami.5b07454
ACS Appl. Mater. Interfaces 2015, 7, 22652−22659

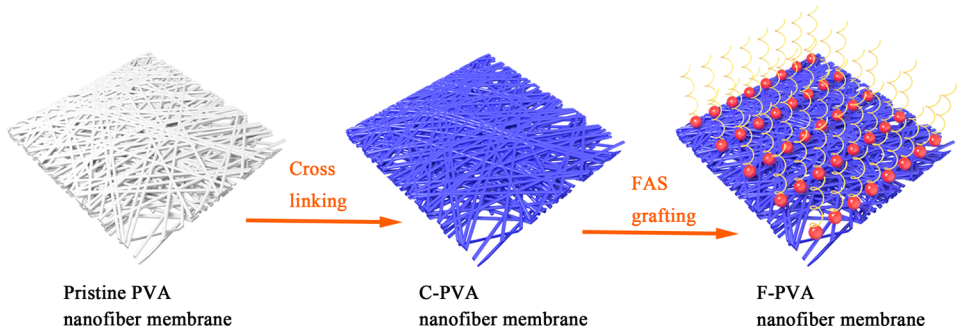

Figure 1. Schematic illustration for the preparation of superhydrophobic F-PVA membrane via cross-linking and FAS grafting.

superhydrophobic PVDF-polytetrafluoroethylene (PTFE) membranes prepared by eletrospinning of PVDF−PTFE blend solutions demonstrated a high and stable permeate flux over a continuous MD test of 15 h with satisfied permeate quality. Liao et al.[18] prepared superhydrophobic PVDF ENMs by surface modification on ENMs with Ag nanoparticles and dodecanethiol, and the resultant superhydrophobic PVDF ENMs displayed antiwetting property during the entire test of 8 h, whereas pristine PVDF ENMs suffered severe pore wetting in less than 1 h.

Although great progress has been made in the preparation of superhydrophobic ENMs via generating a hierarchical structure, the laundering durability of such superhydrophobic membranes in cross-flow operations remains a concern due to the weak adhesion between the nanofibers and nanopartilces. It has been reported that superhydrophobic surfaces with unitary microstructures such as the ramee leaves possess better mechanical properties than those with binary micro- and nanostructures.[20−22] Herein, we describe a new strategy to fabricate ENMs with robust superhydrophobicity by mimicking the unitary microstructures of ramee leaves via eletrospinning of poly(vinyl alcohol) (PVA), followed by chemical cross-linking and surface fluorination. PVA has been selected as the membrane material with respect to its inexpensive cost, excellent chemical stability, and functional hydroxyl groups.[23] For the first time, the robust superhydrophobicity of the ENMs for MD was confirmed under violent ultrasonic treatment and harsh chemical conditions. Additionally, this was the first attempt to utilize hydrophilic polymer instead of hydrophobic polymer to fabricate superhydrophobic ENMs for applications in MD.

2. EXPERIMENTAL SECTION

Material. PVA 1788 was purchased from Shanghai Jinshan Petrochemistry CO. LTD (China) and (Heptadecafluoro-1,1,2,2-tetradecyl) trimethoxysilane (FAS-17) was provided by Nanjing Chengong Organic Silica Materials CO. LTD (China). All other solvents and reagents were produced by Shanghai Sinopharm Chemical Reagent CO. LTD (China) and were used as received. Commercial PTFE flat sheet membranes were purchased from Sumitomo Electric Industries CO. LTD for comparison with the prepared superhydrophobic ENMs.

Preparation of Superhydrophobic FAS-Grafted PVA Nanofiber Membranes. First, certain amount of PVA was dissolved in water with magnetically stirring for at least 1 day at 80 °C to obtain a 10 wt % homogeneous polymer solution. The polymer solution was then electrospun at 1 mL/h with an applied of voltage of 28 kV, and the distance between the needle and collector was set at 15 cm, while the humidity and temperature were maintained at 50 ± 5% and 25 ± 1 °C, respectively.[24] The configuration of the electrospinning setup used in the this study has been detailed in our previous work.[25−28] The pristine PVA nanofiber membranes were subsequently placed in a vacuum oven at 60 °C for at least 1 day to ensure that all solvent have evaporated.

Then, the electrospun PVA membranes were immersed in 0.15 M glutaraldehyde and 0.05 M HCl in acetone solution for 1 h to from a three-dimensional water-resistant network.[24] After that, the membranes were rinsed by water to remove the residue solvents and dried in vacuum at 60 °C for at least 1 day. The cross-linked PVA membranes were labeled as C-PVA membranes.

Finally, the hydrophobic modification process was performed by placing C-PVA nanofiber membranes in a FAS solution (2 wt %) for 1 day. Subsequently, the samples were rinsed by hexane to remove the residual on the surface and dried under vacuum condition at 100 °C for 1 day.[17] The resultant membranes were designated as F-PVA membranes. The schematic illustration for the preparation of superhydrophobic F-PVA membrane via cross-linking and FAS grafting processes is presented in Figure 1.

Membrane Characterization. The chemical composition on membrane surface was analyzed by An X-ray photoelectron spectroscopy analysis (XPS; VG-miclabII, UK). The morphologies and topography of the nanofiber membranes were characterized by scanning electron microscope (SEM; JSM-6360LV, Japan) and Atomic force microscope (AFM; Nanoscope IIIa Multimode, USA), respectively. The WCAs of the membranes were determined by a JC2000D1 system (Shanghai Zhongcheng Digital Technology Apparatus Co. Ltd., China). The water sliding angles of the membranes were measured by gradually tilling the membrane specimen that was fixed on a sample stage from 0 to higher angles and then placing a 10 ul water drop on the stage. The stage angle at which the water drop started to roll off from the membrane surface was denoted as the sliding angle. The membrane porosity was determined by the gravity method reported previously,[29] and the LEPw values were measured using a dead-end filtration setup which was designed according to the method described extensively by Smolders and Franken.[30] The pore sizes of the membranes were characterized by a capillary flow porometer (3H-2000PB, Beijing Beiside Technology Apparatus Co. Ltd., China).

The stability of the superhydrophobicity of the F-PVA nanofiber membranes were tested both in violent mechanical vibration and harsh chemical conditions. The mechanical robustness of the F-PVA membranes was tested by ultrasonication in ethanol for 15, 30, 45, 60 min. The chemical resistance of the F-PVA membranes was examined by placing the F-PVA membranes in corrosive solutions and polar organic solvents including HCl (pH 2), NaOH (pH 12), *N*-methyl-2-pyrrolidone (NMP) and N,N-Dimethylformamide (DMF) for 24, 48, 72, and 96 h.

Vacuum Membrane Distillation. VMD experiments were carried out to evaluate the permeability and antiwetting property of the prepared F-PVA membrane. The VMD system has been detailed in previous studies.[16,17] A 3.5% NaCl solution employed as the feed solution was circulated on the feed side by a pump (90 L/h), with a thermal bath to control its temperature precisely at 333 K. To maintain the feed concentration, desired quantity of deionized water was added based on the weight decrement of the feed tank measured by a digital balance. The water vapor transported through the

DOI: 10.1021/acsami.5b07454
ACS Appl. Mater. Interfaces 2015, 7, 22652−22659

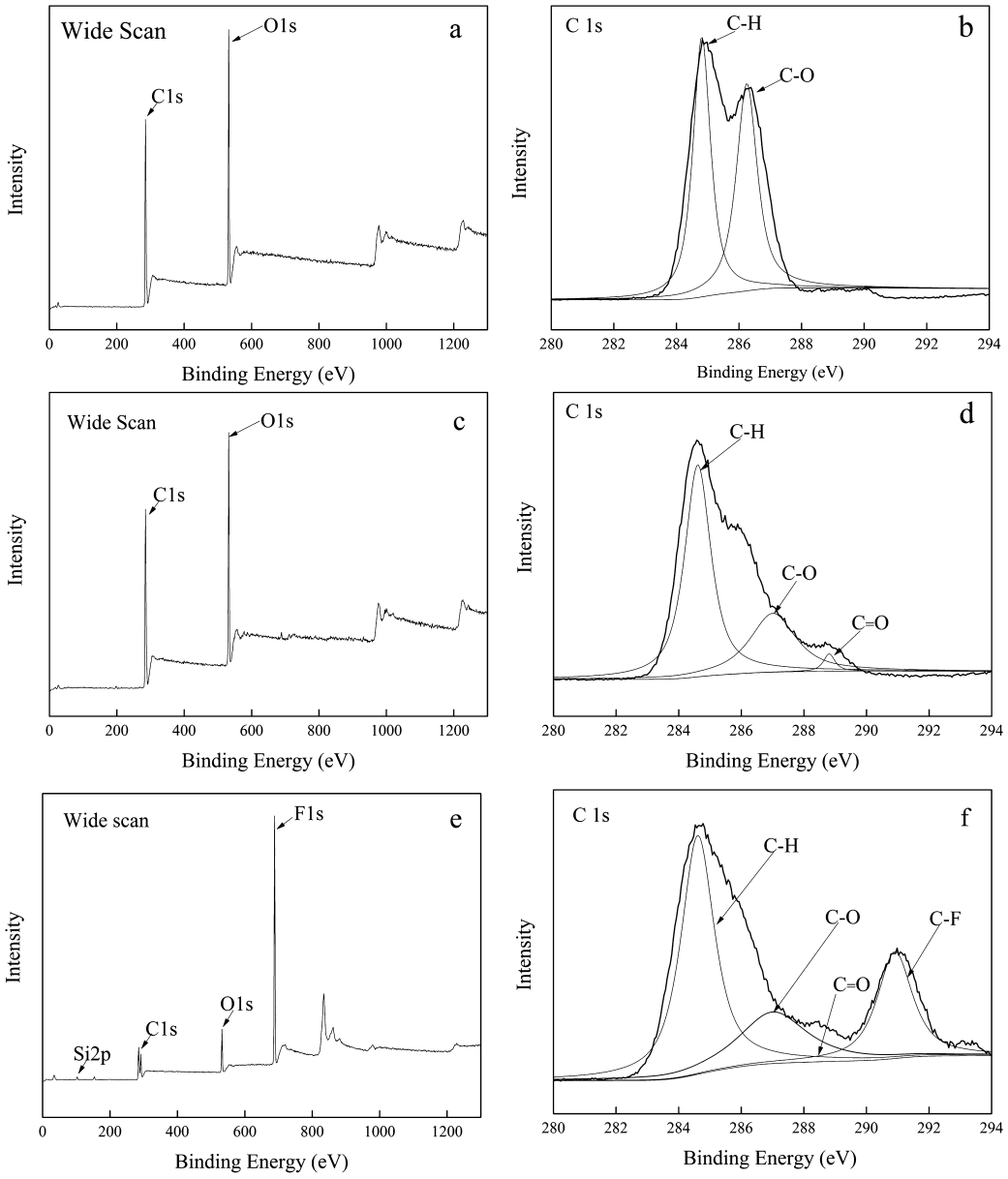

Figure 2. XPS wide-scan and C 1s core level of (a, b) pristine PVA membrane, (c, d) C-PVA membrane, and (e, f) F-PVA membrane.

membrane module to the permeate side and the condensed water was collected in a conical flask, with a vacuum pump to control the permeate pressure at 9 kPa. The permeate flux was measured by the volume of condensed water, and the permeate conductivity was determined by conductivity meters.

3. RESULTS AND DISCUSSION

Chemical Reactions on C-PVA Nanofiber Membrane. The surface chemical compositions of the pristine PVA membrane, cross-linked PVA (C-PVA) membrane and FAS modified PVA (F-PVA) membrane were measured by XPS to investigate the cross-linking and hydrophobic modification process, and the results are shown in Figure 2. Two peaks at binding energy (BE) of 286.4 and 532.7 eV can be seen from the wide-scan spectrum of pristine PVA membrane (Figure 2a), which respectively represents the C 1s and O 1s region. The C1 score-level spectrum of the pristine PVA membrane contains two peak components at 284.6 and 286.4 eV, which separately represent the carbon hydrogen bonding (C−H) and the C−O species from the basic chemical structures of poly(vinyl alcohol). The wide scan of the C-PVA membrane is similar to that of the pristine PVA membrane, indicating that the chemical elements of membrane surface have barely changed after the cross-linking process (Figure 2c). It is worthy noticing that a new peak at 288.8 eV which represents the C═O species appears in the C1 score-level spectrum of the C-PVA membrane (Figure 2d), suggesting that the C-PVA membrane has been successfully cross-linked by glutaraldehyde.

After the FAS modification process, significant changes can be observed on the XPS results of the F-PVA membrane. New peaks at BE of 101.4 and 687.2 eV are presented in the wide-scan spectrum of the F-PVA membrane (Figure 2e), which separately represent Si 2p and F 1s from the FAS molecules. The successful grafting of FAS on the C-PVA membrane is further confirmed by its C 1s core-level line shape. In addition to those peaks observed on the C-PVA membrane, the F-PVA membrane displays another peak at 290.5 eV representing the C−F bonding (Figure 2f), which is ascribed to the grafted FAS

DOI: 10.1021/acsami.5b07454
ACS Appl. Mater. Interfaces 2015, 7, 22652−22659

molecules. On the basis of these XPS information, it can be inferred that a self-assembled FAS monolayer is formed on the surface of the F-PVA membrane due to condensation reactions between the hydroxyl groups on C-PVA membranes and the Si−O alkyl groups in FAS molecules.[31,32]

The surface compositions of the pristine PVA membrane, C-PVA membrane and F-PVA membrane are also tabulated in Table 1. It can be observed that the proportions of C and O elements on the pristine PVA membrane surface almost remained unchangeable after the chemical cross-linking, but then suffered a sharp decline after the FAS grafting. Additionally, the F-PVA membrane presents a high F element content of 48.9%, which could greatly decrease the surface free energy of the nanofiber membrane.

Table 1. Surface Composition of Pristine PVA Membrane, C-PVA Membrane, and F-PVA Membrane

	atom percent (%)			
sample	C 1s	O 1s	F 1s	Si 2p
pristine PVA	69.43	30.57	0.00	0.00
C-PVA	68.08	31.92	0.00	0.00
F-PVA	38.14	10.67	48.87	2.32

Surface Morphology Analysis. Figure 3 presents the surface morphologies of the C-PVA membrane and F-PVA membrane. The C-PVA membrane displays a typical nanofiber fabric surface composed of PVA nanofibers with an average diameter of 182 nm. The nanofiber surface is quite uniform and smooth without observable beads in the SEM images, which is mainly attributed to the optimized eletrospinning conditions. The high voltage (28 kV) employed in this study enhances the elongation force on polymers and accelerates the volatilization of solvents, therefore avoiding beads formation. There is no significant change on the surface morphology of the F-PVA membrane after FAS modification process, concurring with previous reports.[33,34] Besides, the fiber diameter distribution of the F-PVA membrane is similar to that of C-PVA membrane (as shown in Figure S1). This suggests that direct grafting with FAS only changes the surface chemical compositions of the C-PVA membrane without altering its fiber structure.

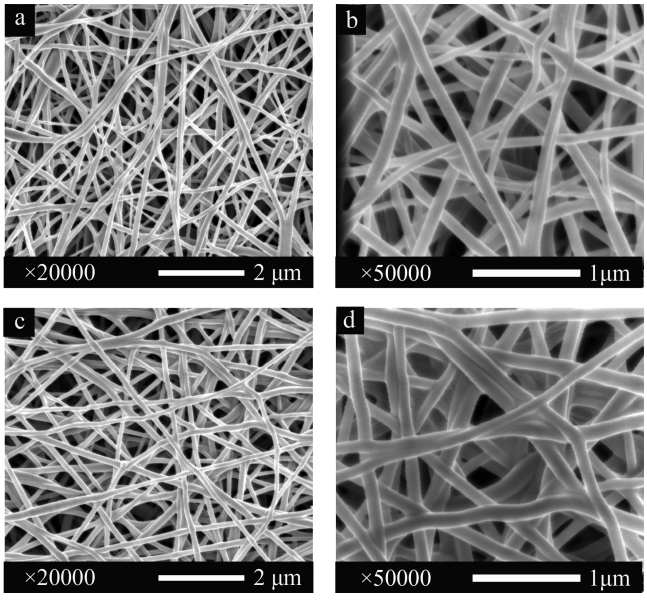

Figure 3. SEM images of (a, b) C-PVA membrane and (c, d) F-PVA membrane with different magnifications.

AFM measurements were also conducted to observe the topography of the C-PVA membrane and F-PVA membrane. As shown in Figure 4, the C-PVA membrane displays a relatively high average surface roughness (Ra) of 118 nm. While conventional membranes fabricated via phase separation process usually possess smooth surface consisting of cellular holes,[35] nanofiber membranes prepared by eletrospinning are made up of randomly distributed nanofibers, which creates ample bumps and results in a highly textured surface.[12] Still, the topography of the F-PVA membrane barely changed after the FAS modification, well corresponding with the SEM results.

Surface Wettability. The water drops on the surfaces of C-PVA membrane and F-PVA membrane and the water contact angles of these membranes are illustrated in Figure 5. The results show that the C-PVA membrane presents a super-hydrophilic surface with a water contact angle of 5.6°. When water was dropped the surface, the water drops were completely absorbed into the membrane in less than 1 s. The superhydrophilicity of the C-PVA membrane is attributed to the abundant OH groups on the surface and the sufficient surface roughness of the membrane. Dramatically, the F-PVA membrane after FAS modification displays a superhydrophobic surface with a water contact angle of 158°. Nearly sphere-like shapes were formed when water was dropped on the membrane surface. The sphere-like drops can readily roll off from the surface with a sliding angle of 4°, indicating its self-cleaning properties.

Although numerous successes have been achieved in the preparation of superhydrophobic surface by mimicking the hierarchical structures of lotus leaves, it has been proved that surfaces with unitary microstructures can also possess self-cleaning properties with high contact angles and sliding angles by mimicking the unique structure of ramee leaves.[20] The surface of F-PVA membrane consisting of randomly distributed nanofibers resembles the fabric surface of ramee leaves, which provides sufficient roughness to create abundant air pockets on membrane surface. Furthermore, the C and F element separately accounts for 38.1% and 48.9% on the surface composition of the F-PVA membrane (Table 1), indicating its extremely low surface energy. Therefore, the unitary micro-structure of smooth nanofibers and the low surface energy altogether construct the self-cleaning properties of the F-PVA membrane.

The effect of the FAS modification process on surface hydrophobicity of the F-PVA membrane was also investigated by varying the concentration of FAS solutions in grafting process. The results reveal that the increase of FAS concentration leads to a gradually increase of the water contact angle of F-PVA membrane (see Figure S2), indicating that the FAS modification process plays a key role in the generation of surface superhydrophobicity.

Mechanical and Chemical Stability. As mentioned previously, the long-term stability of the superhydrophobic membranes remains a challenge for their practical applications. It is expected that the F-PVA nanofiber membrane could possess robust superhydrophobicity with respect to its unique unitary microstructure.

The F-PVA membrane was first tested under violent mechanical vibration by ultrasonication for 60 min, and the variation of water contact angle and sliding angles is shown in

DOI: 10.1021/acsami.5b07454
ACS Appl. Mater. Interfaces 2015, 7, 22652−22659

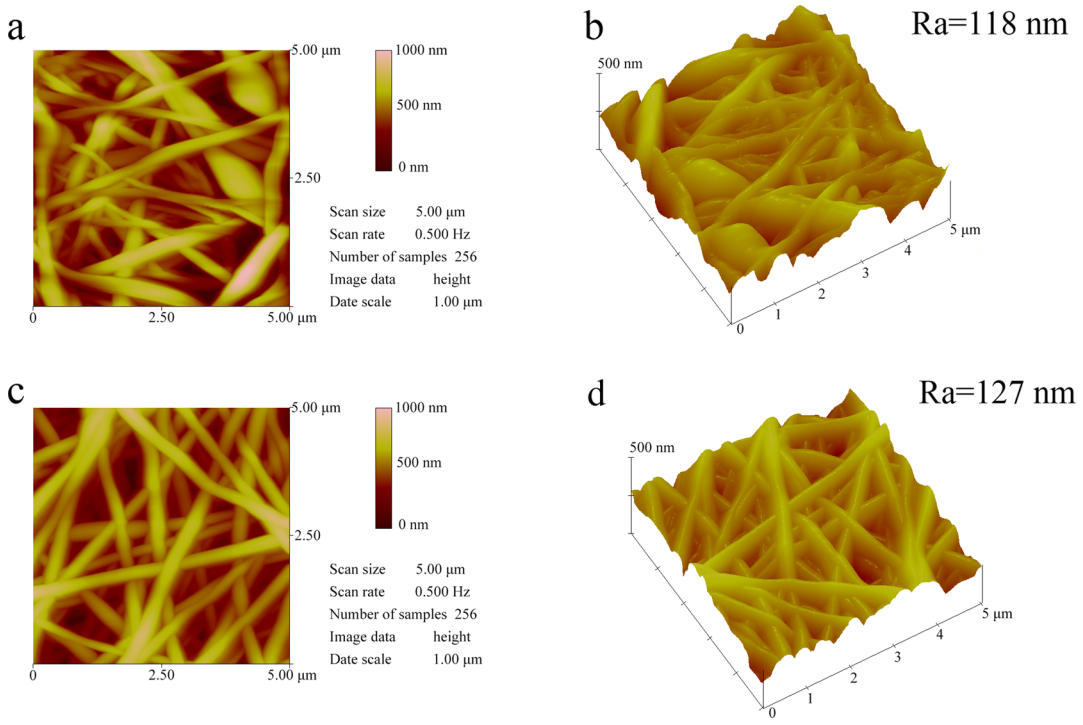

Figure 4. 2D and 3D AFM images of (a, b) C-PVA membrane and (c, d) F-PVA membrane.

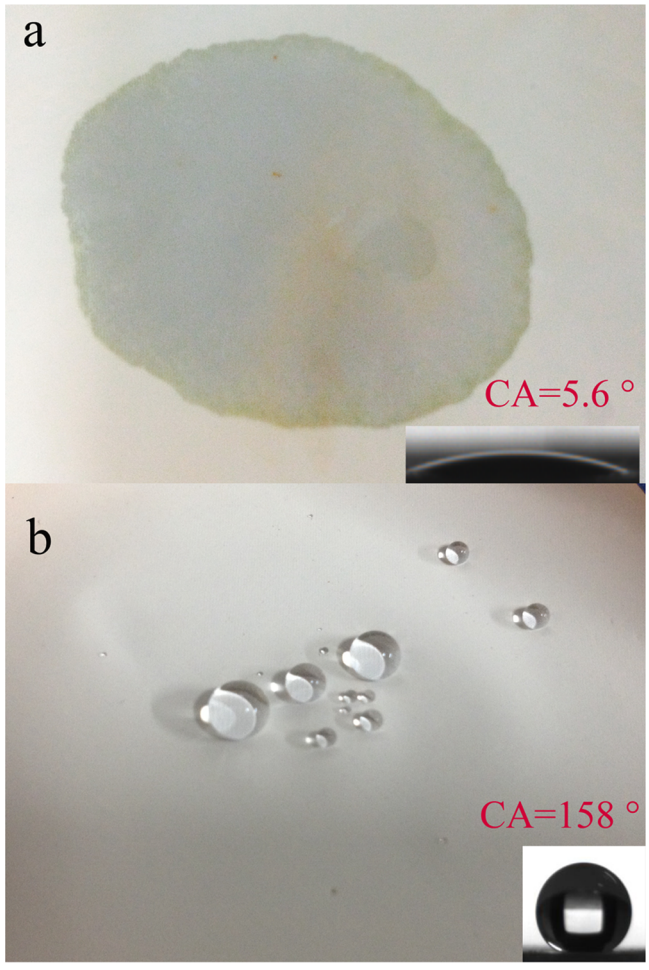

Figure 5. Water drops on the surfaces of (a) C-PVA membrane and (b) F-PVA membrane.

Figure 6. The results show that the water contact angle and sliding angle of the F-PVA membrane changed slightly from

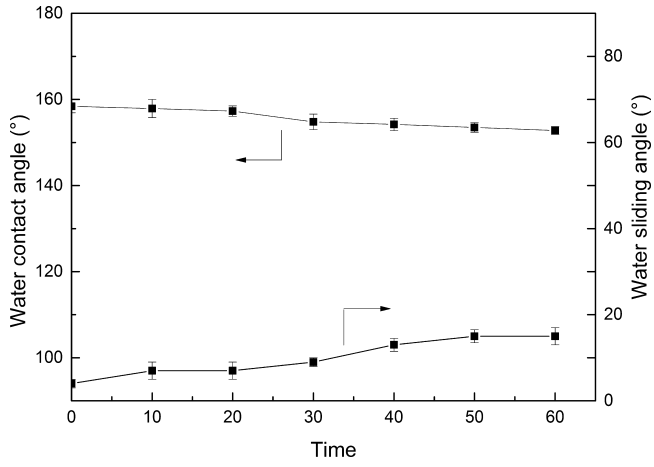

Figure 6. Variation of water contact angle and sliding angle of F-PVA nanofiber membrane with time under ultrasonication.

158 to 153° and 4 to 15° over the entire test, respectively. This result indicates that the chemical bonding force of Si−O alkyl groups on the F-PVA membrane surface is strong enough to maintain its superhydrophobicity under violent mechanical vibration.

The chemical resistance of the F-PVA membrane was also tested in corrosive solutions and polar organic solvents and results are summarized in Figure 7. The water contact angle of the F-PVA membrane barely changed after being immersed in these chemical solvents for a period of 96 h, suggesting its great chemical resistance. The cross-linking reaction of PVA renders the C-PVA membrane satisified chemical stability to water and most organic solvents. Besides, due to the chemical inertness of the C−C and C−F bondings in the FAS molecular, the F-PVA

DOI: 10.1021/acsami.5b07454
ACS Appl. Mater. Interfaces 2015, 7, 22652−22659

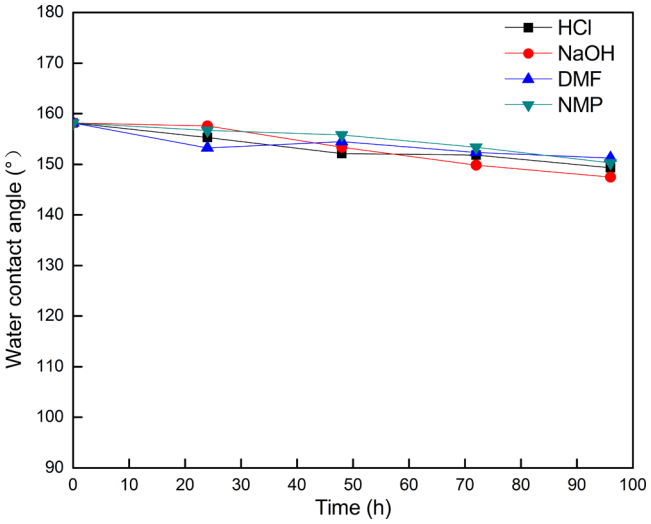

Figure 7. Variation of water contact angle of F-PVA nanofiber membrane with time under harsh chemical conditions.

membrane after FAS modification can retain its superhydrophobicity in harsh chemical conditions.

Membrane Structure. The common characteristics of the superhydrophobic F-PVA naofiber membrane and a commercial PTFE membrane are listed in Table 2. The results show

Table 2. Characteristic Properties of F-PVA Membrane and Commercial PTFE

membrane code	F-PVA	commercial PTFE
thickness (μm)	100 ± 3	81 ± 1
porosity (%)	82 ± 2	55 ± 1
mean pore size (μm)	0.46 ± 0.01	0.29 ± 0.01
max pore size (μm)	0.54 ± 0.02	0.42 ± 0.01
water contact angle (deg)	158 ± 2.0	121.5 ± 1.0
LEPw (kPa)	179 ± 3	125 ± 2

that the F-PVA nanofiber membrane displays a significantly higher porosity (82%) than the commercial PTFE membrane (55%). Distinguishing from the tortuous pore structures of commercial membranes via phase inversion or stretching, the interconnected open structures of electrospun nanofiber membranes lead to their higher porosity.

Figure 8 illustrates the pore size distributions of the F-PVA membrane and the commercial PTFE membrane. The F-PVA membrane presents a narrow distribution of pore diameter ranging from 0.38 to 0.54 μm, which is mainly attributed to the fine fiber diameter distribution (see Figure S1). The commercial PTFE membrane exhibits a slightly broader pore size distribution with pore diameter in the range of 0.22 to 0.42 μm. The pore size range and distribution are key factors influencing the vapor flux and permeation quality in MD processes, and it is suggested that a membrane with a narrow distribution of pore size ranging from 0.2 to 0.5 μm is preferred according to the Knudsen and viscous diffusion theory.[9] Therefore, both the F-PVA membrane and commercial PTFE membrane exhibit desirable pore sizes for VMD applications.

The LEPw values were also measured to evaluate the membrane wetting resistance. It can be observed from Table 2 that the F-PVA membrane presents a higher LEPw value of 179 kPa than the commercial PTFE membrane (125 kPa), regardless of its relative larger pore size. This is mainly ascribed

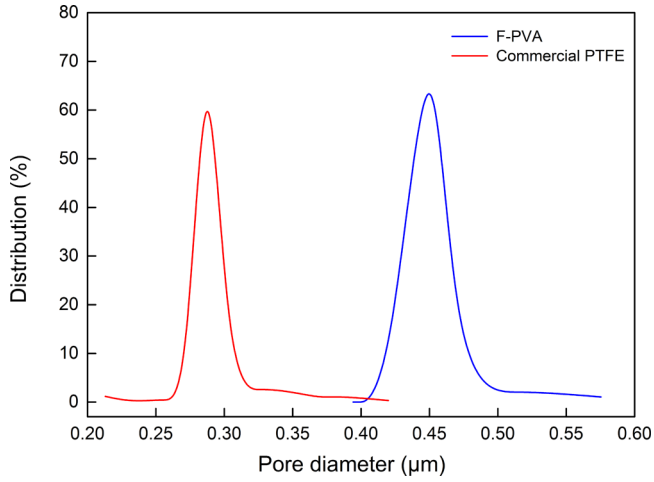

Figure 8. Pore size distribution of F-PVA membrane and commercial PTFE.

to the superhydrophobicity of the F-PVA membrane with a high water contact angle of 158°, which creates sufficient air pockets on membrane surface and effectively improves the water penetrating resistance of the membrane. The LEPw value of the F-PVA membrane is remarkable, because most electrospun nanofiber membranes used in MD possessed LEPw values lower than 100 kPa.[13,15]

VMD Performance. To explore the potential of the superhydrophobic F-PVA nanofiber membrane in MD applications, we conducted continuous VMD experiments to evaluate the permeability and wetting resistance of the superhydrophobic F-PVA nanofiber membrane and the commercial PTFE flat sheet membrane.

It can be seen from Figure 9 that the permeate flux of the F-PVA nanofiber membrane was about 25.2 kg/m^{2}h, which was

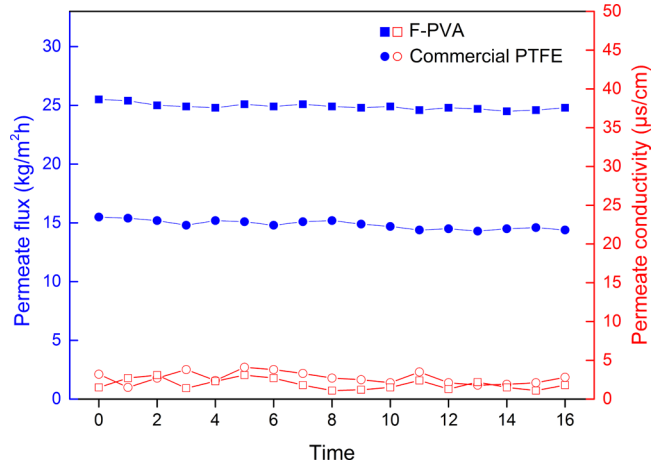

Figure 9. Continuous VMD tests of F-PVA nanofiber membrane and commercial PTFE membrane (35 g/L NaCl solution as the feed, feed temperature = 333 K, permeate pressure = 9 kPa flow rate = 90 L/h).

almost 70% higher than that of the commercial PTFE membrane. The F-PVA nanofiber possessed a relative larger mean pore size and a higher porosity than the commercial PTFE membrane, therefore a notably higher permeate flux was attained regardless of its thicker thickness. Besides, Figure 9 also illustrates that the F-PVA and commercial PTFE membrane both maintained a stable flux with desirable

DOI: 10.1021/acsami.5b07454
ACS Appl. Mater. Interfaces 2015, 7, 22652−22659

permeate conductivity (<5 μs/cm) over the entire test, which was mainly attributed to their high LEPw values (>120 kPa).

The VMD test suggests that the F-PVA nanofiber membrane can maintain a remarkable permeate flux with satisfied permeate quality over the long-term stage, indicating its promising potentials for practical applications.

4. CONCLUSIONS

In summary, we have developed a novel type of ENMs with robust superhydrophobicity for MD process via eletrospinning of PVA followed by chemical cross-linking and surface fluorination. The XPS information confirms that the FAS molecular has been successfully grafted on the surface of cross-linked PVA nanofiber membrane, while the SEM and AFM results reveal that the membrane structure has seldom changed after the FAS modification. The result F-PVA membrane displays robust superhydrophobicty under violent ultrasonic treatment and harsh chemical conditions. Furthermore, the VMD tests illustrate that the F-PVA membrane present a stable and high permeate flux of 25.2 kg/(m^2 h) with satisfied permeate conductivity due to its interconnected open structure and robust superhydrophobicity, suggesting its great potentials for the application of MD process.

■ ASSOCIATED CONTENT

Supporting Information

The Supporting Information is available free of charge on the ACS Publications website at DOI: 10.1021/acsami.5b07454.

Fiber diameter distribution of C-PVA membrane and F-PVA membrane (Figure S1); effect of FAS concentration on the water contact angle of F-PVA nanofiber membrane (Figure S2) (PDF)

■ AUTHOR INFORMATION

Corresponding Author

*E-mail: chemxuzl@ecust.edu.cn. Tel: 86-21-64253670.

Notes

The authors declare no competing financial interest.

■ ACKNOWLEDGMENTS

The authors are thankful for financial support by the National Natural Science Foundation of China (21176067 and 21406060).

■ REFERENCES

(1) Ghaffour, N.; Missimer, T. M.; Amy, G. L. Technical Review and Evaluation of the Economics of Water Desalination: Current and Future Challenges for Better Water Supply Sustainability. *Desalination* **2013**, *309*, 197−207.

(2) Elimelech, M.; Phillip, W. A. The Future of Seawater Desalination: Energy, Technology, and the Environment. *Science* **2011**, *333*, 712−717.

(3) Drioli, E.; Ali, A.; Macedonio, F. Membrane Distillation: Recent Developments and Perspectives. *Desalination* **2015**, *356*, 56−84.

(4) Wang, P.; Chung, T.-S. Recent Advances in Membrane Distillation Processes: Membrane Development, Configuration Design and Application Exploring. *J. Membr. Sci.* **2015**, *474*, 39−56.

(5) Gethard, K.; Sae-Khow, O.; Mitra, S. Water Desalination Using Carbon-Nanotube-Enhanced Membrane Distillation. *ACS Appl. Mater. Interfaces* **2011**, *3*, 110−114.

(6) Shirazi, M. M. A.; Kargari, A.; Tabatabaei, M. Evaluation of Commercial Ptfe Membranes in Desalination by Direct Contact Membrane Distillation. *Chem. Eng. Process.* **2014**, *76*, 16−25.

(7) Khayet, M. Membranes and Theoretical Modeling of Membrane Distillation: A Review. *Adv. Colloid Interface Sci.* **2011**, *164*, 56−88.

(8) Wang, P.; Chung, T. S. A New-Generation Asymmetric Multi-Bore Hollow Fiber Membrane for Sustainable Water Production Via Vacuum Membrane Distillation. *Environ. Sci. Technol.* **2013**, *47*, 6272−6278.

(9) Phattaranawik, J. Effect of Pore Size Distribution and Air Flux on Mass Transport in Direct Contact Membrane Distillation. *J. Membr. Sci.* **2003**, *215*, 75−85.

(10) Guo, F.; Servi, A.; Liu, A.; Gleason, K. K.; Rutledge, G. C. Desalination by Membrane Distillation Using Electrospun Polyamide Fiber Membranes with Surface Fluorination by Chemical Vapor Deposition. *ACS Appl. Mater. Interfaces* **2015**, *7*, 8225−8232.

(11) Zhou, T.; Yao, Y.; Xiang, R.; Wu, Y. Formation and Characterization of Polytetrafluoroethylene Nanofiber Membranes for Vacuum Membrane Distillation. *J. Membr. Sci.* **2014**, *453*, 402−408.

(12) Tijing, L. D.; Choi, J.-S.; Lee, S.; Kim, S.-H.; Shon, H. K. Recent Progress of Membrane Distillation Using Electrospun Nanofibrous Membrane. *J. Membr. Sci.* **2014**, *453*, 435−462.

(13) Maab, H.; Francis, L.; Al-saadi, A.; Aubry, C.; Ghaffour, N.; Amy, G.; Nunes, S. P. Synthesis and Fabrication of Nanostructured Hydrophobic Polyazole Membranes for Low-Energy Water Recovery. *J. Membr. Sci.* **2012**, *423−424*, 11−19.

(14) Feng, C.; Khulbe, K. C.; Matsuura, T.; Gopal, R.; Kaur, S.; Ramakrishna, S.; Khayet, M. Production of Drinking Water from Saline Water by Air-Gap Membrane Distillation Using Polyvinylidene Fluoride Nanofiber Membrane. *J. Membr. Sci.* **2008**, *311*, 1−6.

(15) Liao, Y.; Wang, R.; Tian, M.; Qiu, C.; Fane, A. G. Fabrication of Polyvinylidene Fluoride (Pvdf) Nanofiber Membranes by Electro-Spinning for Direct Contact Membrane Distillation. *J. Membr. Sci.* **2013**, *425−426*, 30−39.

(16) Dong, Z.-Q.; Ma, X.-h.; Xu, Z.-L.; You, W.-T.; Li, F.-b. Superhydrophobic Pvdf−Ptfe Electrospun Nanofibrous Membranes for Desalination by Vacuum Membrane Distillation. *Desalination* **2014**, *347*, 175−183.

(17) Dong, Z.-Q.; Ma, X.-H.; Xu, Z.-L.; Gu, Z.-Y. Superhydrophobic Modification of Pvdf-SiO_2 Electrospun Nanofiber Membranes for Vacuum Membrane Distillation. *RSC Adv.* **2015**, *5*, 67962−67970.

(18) Liao, Y.; Wang, R.; Fane, A. G. Engineering Superhydrophobic Surface on Poly(Vinylidene Fluoride) Nanofiber Membranes for Direct Contact Membrane Distillation. *J. Membr. Sci.* **2013**, *440*, 77−87.

(19) Li, X.; Wang, C.; Yang, Y.; Wang, X.; Zhu, M.; Hsiao, B. S. Dual-Biomimetic Superhydrophobic Electrospun Polystyrene Nanofibrous Membranes for Membrane Distillation. *ACS Appl. Mater. Interfaces* **2014**, *6*, 2423−2430.

(20) Guo, Z.; Liu, W. Biomimic from the Superhydrophobic Plant Leaves in Nature: Binary Structure and Unitary Structure. *Plant Sci.* **2007**, *172*, 1103−1112.

(21) Zhu, H.; Guo, Z. A Superhydrophobic Copper Mesh with Microrod Structure for Oil-Water Separation Inspired from Ramee Leaf. *Chem. Lett.* **2014**, *43*, 1645−1647.

(22) Wang, G.; Wang, H.; Guo, Z. A Robust Transparent and Anti-Fingerprint Superhydrophobic Film. *Chem. Commun.* **2013**, *49*, 7310−7312.

(23) Wang, X.; Chen, X.; Yoon, K.; Fang, D.; Hsiao, B. S.; Chu, B. High Flux Filtration Medium Based on Nanofibrous Substrate with Hydrophilic Nanocomposite Coating. *Environ. Sci. Technol.* **2005**, *39*, 7684−7691.

(24) Liu, Y.; Wang, R.; Ma, H.; Hsiao, B. S.; Chu, B. High-Flux Microfiltration Filters Based on Electrospun Polyvinylalcohol Nanofibrous Membranes. *Polymer* **2013**, *54*, 548−556.

(25) Lu, P. P.; Xu, Z. L.; Yang, H.; Wei, Y. M. Processing-Structure-Property Correlations of Polyethersulfone/Perfluorosulfonic Acid Nanofibers Fabricated Via Electrospinning from Polymer-Nanoparticle Suspensions. *ACS Appl. Mater. Interfaces* **2012**, *4*, 1716−1723.

(26) Lu, P.-P.; Xu, Z.-L.; Yang, H.; Wei, Y.-M.; Xu, H.-T. Effects of Ethanol and Isopropanol on the Structures and Properties of

DOI: 10.1021/acsami.5b07454
ACS Appl. Mater. Interfaces 2015, 7, 22652−22659

Polyethersulfone/Perfluorosulfonic Acid Nanofibers Fabricated Via Electrospinning. *J. Polym. Res.* **2012**, *19*, 9854−9864.
(27) Lu, P.-P.; Xu, Z.-L.; Yang, H.; Wei, Y.-M. Preparation and Characterization of High-Performance Perfluorosulfonic Acid/SiO_2 nanofibers with Catalytic Property Via Electrospinning. *Ind. Eng. Chem. Res.* **2012**, *51*, 11348−11354.
(28) Ma, X.-H.; Dong, Z.-Q.; Zhang, P.-Y.; Zhong, Q.-F.; Xu, Z.-L. Preparation and Characterization of Superhydrophilic Pvdf Electrospun Nanofibrous Membrane Based on in Situ Free Radical Polymerization. *Mater. Lett.* **2015**, *156*, 58−61.
(29) Lawson, K. W.; Lloyd, D. R. Membrane Distillation. *J. Membr. Sci.* **1997**, *124*, 1−25.
(30) SMOLDERS, K.; FRANKEN, A. C. M. Terminology for Membrane Distillation. *Desalination* **1989**, *72*, 249−262.
(31) Kujawa, J.; Kujawski, W.; Koter, S.; Jarzynka, K.; Rozicka, A.; Bajda, K.; Cerneaux, S.; Persin, M.; Larbot, A. Membrane Distillation Properties of TiO_2 ceramic Membranes Modified by Perfluoroalkylsilanes. *Desalin. Water Treat.* **2013**, *51*, 1352−1361.
(32) Krajewski, S.; Kujawski, W.; Bukowska, M.; Picard, C.; Larbot, A. Application of Fluoroalkylsilanes (Fas) Grafted Ceramic Membranes in Membrane Distillation Process of Nacl Solutions. *J. Membr. Sci.* **2006**, *281*, 253−259.
(33) Fang, H.; Gao, J. F.; Wang, H. T.; Chen, C. S. Hydrophobic Porous Alumina Hollow Fiber for Water Desalination Via Membrane Distillation Process. *J. Membr. Sci.* **2012**, *403*−*404*, 41−46.
(34) Koonaphapdeelert, S.; Li, K. Preparation and Characterization of Hydrophobic Ceramic Hollow Fibre Membrane. *J. Membr. Sci.* **2007**, *291*, 70−76.
(35) Guillen, G. R.; Pan, Y.; Li, M.; Hoek, E. M. V. Preparation and Characterization of Membranes Formed by Nonsolvent Induced Phase Separation: A Review. *Ind. Eng. Chem. Res.* **2011**, *50*, 3798−3817.

DOI: 10.1021/acsami.5b07454
ACS Appl. Mater. Interfaces 2015, 7, 22652−22659